

1
2
3
4
5
6
7
8
9
10
11
12
13
14
15
16
17
18
19
20
21
22
23
24
25
26

Title:

A new highly sensitive and specific real-time PCR assay targeting the malate dehydrogenase gene of *Kingella kingae* and application to 201 pediatric clinical specimens

Running title (52<54 characters and spaces):

A new real-time PCR targeting the *K. kingae mdh* gene

Authors:

Nawal El Houmami^{1#}, MD, PhD; Guillaume André Durand¹, MD, MSc; Janek Bzdrenga², PhD; Anne Darmon¹, MD, MSc; Philippe Minodier³, MD, MSc; Hervé Seligmann¹, PhD; Didier Raoult¹, MD, PhD; Pierre-Edouard Fournier^{1#}, MD, PhD

Authors' affiliations :

¹UMR VITROME, Aix-Marseille Univ, IRD, Service de Santé des Armées, Assistance Publique-Hôpitaux de Marseille, Institut Hospitalo-Universitaire Méditerranée-Infection, Marseille, France.

²Univ. Grenoble-Alpes, CEA, CNRS, IBS, F-38000, Grenoble, France.

³Department of Pediatric Emergency Medicine, North Hospital, Marseille, France.

Corresponding authors :

#Dr. Nawal El Houmami, UMR VITROME, Institut Hospitalo-Universitaire Méditerranée Infection, Assistance Publique-Hôpitaux de Marseille, 19-21 Boulevard Jean Moulin, 13005 Marseille, France.

[\[nawal.el-houmami@etu.univ-amu.fr\]](mailto:nawal.el-houmami@etu.univ-amu.fr).

#Prof. Pierre-Edouard Fournier, UMR VITROME, Institut Hospitalo-Universitaire Méditerranée-Infection, 19-21 Boulevard Jean Moulin, 13005 Marseille, France. [\[pierre-edouard.fournier@univ-](mailto:pierre-edouard.fournier@univ-amu.fr)

[amu.fr\]](mailto:pierre-edouard.fournier@univ-amu.fr).

Telephone: + (33) 413 732 401, Fax: + (33) 413 732 402.

27 **ABSTRACT**

28 *Kingella kingae* is a significant pediatric pathogen responsible for bone and joint infections, occult
29 bacteremia, and endocarditis in early childhood. Past efforts to detect this bacterium by culture and
30 broad-range 16S rRNA gene polymerase chain reaction (PCR) assays from clinical specimens have
31 proven unsatisfactory and were gradually let out for the benefit of specific real-time
32 PCR tests targeting the *groEL* gene and RTX locus of *K. kingae* by the late 2000s. However, recent
33 studies showed that real-time PCR (RT-PCR) assays targeting the *Kingella* sp. RTX locus that are
34 currently available for the diagnosis of *K. kingae* infection lack of specificity because they could not
35 distinguish between *K. kingae* and the recently described *K. negevensis* species. Furthermore, in
36 silico analysis of the *groEL* gene from a large collection of 45 *K. kingae* strains showed that primers
37 and probes from *K. kingae groEL*-based RT-PCR assays display a few mismatches with *K. kingae*
38 *groEL* variations that may result in a decreased detection sensitivity, especially in paucibacillary
39 clinical specimens. In order to provide an alternative to *groEL*- and RTX-targeting RT-PCR assays that
40 may suffer from suboptimal specificity and sensitivity, a *K. kingae*-specific RT-PCR assay targeting the
41 malate dehydrogenase (*mdh*) gene was developed for predicting no mismatch against 18 variants
42 of the *K. kingae mdh* gene from 20 distinct sequences types of *K. kingae*. This novel *K. kingae*-specific
43 RT-PCR assay demonstrated a high specificity and sensitivity and was successfully used to diagnose *K.*
44 *kingae* infections and carriage in 104 clinical specimens from children aged between 7 months and 7
45 years old.

46

47

48

49

50

51

52

53 **INTRODUCTION**

54 *Kingella kingae* is a significant pediatric pathogen responsible for bone and joint infections, occult
55 bacteremia and, more rarely, endocarditis that may occur either sporadically, or in the context of
56 outbreaks in daycare centers [1,2]. Past efforts to detect this organism by culture have proven
57 unsatisfactory and molecular diagnostics were gradually used in the 2000s to successfully diagnose *K.*
58 *kingae* disease [3-5]. Consequently, the increasing number of molecularly-confirmed *K. kingae*
59 infections in infants led to this organism being recognized as the primary agent of septic arthritis,
60 osteomyelitis, and tenosynovitis in children aged between six and 36 months in countries where *K.*
61 *kingae*-specific real-time PCR assays are routinely employed [4-7]. This contributed to significantly
62 improve our knowledge of the etiology of infantile bone and joint infections [5, 8, 9]. In addition to
63 increasing the detection yield of microorganisms from osteoarticular samples, molecular assays have
64 contributed to a better understanding of the epidemiology of *K. kingae* carriage among healthy
65 carriers and ill children [10-12]. Although polymerase chain reaction (PCR) assays targeting the 16S
66 rRNA gene made it possible to moderately enhance the detection of the organism from
67 osteoarticular samples [13], the development of *K. kingae*-specific RT-PCR assays allowed a
68 substantial increase in the diagnosis of *K. kingae* infections and oropharyngeal carriage [5,14,15].
69 To date, only the *groEL* (also known as *cpn60*) gene and those located in the RTX locus, namely *rtxA*
70 and *rtxB*, have been targeted for the development of *K. kingae*-specific RT-PCR assays [4,5,16,17].
71 Comprehensively studied, the *groEL* gene encodes a chaperone protein that is considered as a
72 universal bacterial marker [18], and PCR assays targeting this gene are widely used for the molecular
73 diagnosis of infectious diseases [19-21]. However, although recent studies have confirmed that
74 targeting the *groEL* gene from *K. kingae* (*KkigroEL*) is a reliable strategy for the molecular detection
75 of this bacterium in clinical specimens [15,22], primers and probes from *groEL*-based RT-PCR assays
76 that were reported by Ilharreborde *et al.* [4] and Levy *et al.* [5] display a few mismatches with
77 *KkigroEL* variations that may result in a decreased detection sensitivity [15, 23].

78 In contrast, RTX-targeting RT-PCR assays gained great popularity worldwide because they were
79 initially believed to be highly specific for *K. kingae* [16,17]. However, the RTX locus of *K. kingae* is
80 flanked by mobile genetic elements that are present in genomic regions of decreased GC content
81 (30% versus an average of 46.6% for the whole genome of *K. kingae*). Because such a GC content
82 difference is a meaningful genetic marker of mobilome, Kehl-Fie *et al.* suggested that this RTX locus
83 was horizontally-acquired [24]. This assumption was recently confirmed by the presence of an
84 identical RTX locus in the genome of *K. negevensis* [15,25], a newly described *Kingella* species
85 isolated from the oropharynxes of Israeli and Swiss children [26,27], and from the vaginal discharge
86 of a young woman [25]. Furthermore, *in vitro* studies indicated that RT-PCR assays targeting the RTX
87 locus of *K. kingae* were also positive for *K. negevensis* and, hence, could not formally discriminate
88 both species when used alone [15]. *Kingella negevensis* has also been identified in the hip of an 8-
89 month-old boy with a specific qPCR targeting the *K. negevensis groEL* gene, indicating that this novel
90 described *Kingella* species may occasionally be a pediatric pathogen [15].
91 In order to provide an alternative to *groEL*- and RTX-targeting RT-PCR assays that may suffer from
92 suboptimal specificity and sensitivity, a *K. kingae*-specific RT-PCR assay targeting the malate
93 dehydrogenase (*mdh*) gene, a housekeeping gene, was developed. This novel RT-PCR assay targeting
94 the *mdh* gene from *K. kingae* (*Kkimdh*) demonstrated a high specificity and sensitivity and was
95 successfully used to diagnose *K. kingae* infections and carriage in 104 clinical specimens from young
96 children.

97

98

99 MATERIALS AND METHODS

100 **Bacterial isolates.** In the 2000s, epidemiological studies were conducted in southern Israel on 7,217
101 healthy children, from whom *K. kingae* strains were isolated at the Soroka University Medical Center,
102 Beer-Sheva, Israel [26]. Forty of these *K. kingae* strains, cultivated from children aged between six
103 and 48 months suffering from osteoarticular infections (n=12), occult bacteremia (n=4), endocarditis

104 (n=3), or asymptomatic oropharyngeal colonization (n=21), were used in this study (Table S1).
105 Oropharyngeal swabs from healthy children were first inoculated onto a selective vancomycin-
106 containing agar (also named BAV medium) to inhibit the competing Gram-positive flora and facilitate
107 the recognition of hemolytic *K. kingae* colonies [28]. All *K. kingae* isolates were then subcultured on
108 5% sheep blood-enriched Columbia agar for between 24 and 36 hours at 37°C in a 5% CO₂-enriched
109 atmosphere. Additionally, 86 other bacterial strains, including all other *Kingella* species, namely *K.*
110 *negevensis* strain Sch538^T, *K. oralis* CIP103803^T, *K. denitrificans* CIP103473^T and *K. potus* CIP108935^T,
111 as well as members of the *Neisseria*, *Haemophilus*, *Staphylococcus*, *Streptococcus* and
112 *Mycobacterium* genera, were used to determine the specificity of the RT-PCR primers and probes
113 targeting the *Kkimdh* gene (Table S2).

114 **Clinical specimens of *K. kingae* infection and carriage.** Between December 2013 and December
115 2017, 106 children with *K. kingae* infections and/or carriage originally from Europe, South America,
116 Africa, and the South Pacific, were diagnosed by using *KkigroEL*-specific RT-PCR [5] at the IHU
117 Méditerranée-Infection, Marseille, France. Of those, 96 clinical specimens or extracted DNA (from 95
118 children) that were stored at -80°C were retrieved, which were derived from joint fluid (n=64), bone
119 tissue (n= 6), tenosynovial fluid (n=2), soft tissue (n=2), endocardial cushion (n=1), and pharyngeal
120 swab (n=25) (Table S3). The efficiency of DNA extraction and the possible presence of inhibitors were
121 evaluated in all clinical specimens using the RS42-Km primer pair that targets a fragment of the
122 human β-globin gene [5].

123 **Genomic DNA extraction.** Genomic DNA from all bacterial strains and clinical samples was extracted
124 with a BioRobot EZ1 workstation and an EZ1 DNA tissue kit (Qiagen, Courtaboeuf, France) according
125 to the manufacturer's recommendations [15]. DNA was stored at -80°C prior to molecular assays. To
126 limit the effects of PCR inhibitors, all extracted DNAs were tested both undiluted and diluted 1:10.

127 **Selection of the *mdh* gene from *K. kingae* genomes.** In order to select a relevant target gene for the
128 development of a *K. kingae*-specific RT-PCR assay, a comparison of five *K. kingae* genomes available
129 in GenBank, namely *K. kingae* ATCC 23330^T (FOJK01000000) [26], *K. kingae* KKWG1 (LN869922) [29],

130 *K. kingae* PYKK081 (NZ_JH621344), *K. kingae* 11220434 (JH768595) [30] and *K. kingae* KK247
131 (CCJT01000000) [31], was performed using the Geneious R11.0.5 software
132 (<http://www.geneious.com>) [32]. Genes and their flanking regions belonging to the core genome of
133 *K. kingae* and exhibiting a GC content close to 50% were screened to facilitate the primer and probe
134 design according to the Takyon polymerase protocol (Eurogentec, Seraing, Belgium). The *mdh* gene
135 of *K. kingae* (*Kkimdh*) coding the malate dehydrogenase met the above criteria and was thus
136 selected. Thereafter, paired-end sequencing of the *Kkimdh* gene and its flanking regions from 40 *K.*
137 *kingae* strains using a MiSeq sequencer (Illumina Inc., San Diego, CA, USA), as well as genome
138 assembly, were performed as previously described [26].

139 **Characterization of the *Kingella kingae mdh* gene.** A MAFFT alignment of the *Kkimdh* nucleotide
140 sequences and its flanking regions from the 45 studied *K. kingae* strains was performed using
141 Geneious R11.0.5 [32,33]. The related distance matrix of the 45 distinct *Kkimdh* genes was obtained
142 using Geneious R11.0.5 (Table S4). To detect possible lateral gene transfer from or within the
143 genome of other bacterial species, a megablastn search with default parameters
144 (<http://blast.ncbi.nlm.nih.gov>) was then conducted by comparing the obtained *mdh* orthologous
145 sequences and their genomic environment to public databases. A neighbor-joining tree of *Kkimdh*
146 gene sequences was then created using MEGA7 with default parameters [34].

147 **RT-PCR assay targeting the *Kkimdh* gene. (a) Design of primers and probe.** To design specific
148 primers and probes, a MAFFT alignment of *mdh* nucleotide sequences from the 45 studied *K. kingae*
149 strains was first performed. Thereafter, the primers Fwd_*Kkimdh* (5- TGTTCCGCATTGCTTCTG -3) and
150 Rev_*Kkimdh* (5- TCATGCCGTCCAACAATG -3) amplifying a 144-bp fragment, and the probe P_*Kkimdh*
151 (5- 6-carboxyfluorescein [FAM]- CATCATCACGCCCTGAACGGCTT -3) were manually designed.
152 Particular care was taken in order to avoid nucleotide mismatches between all *K. kingae* strains, and
153 to maximize mismatches with *mdh* orthologous detected from other bacterial species. Primers and
154 probe specificity was confirmed in silico using the BLAST tool (<http://blast.ncbi.nlm.nih.gov>).

155 **(b) *Kkimdh* RT-PCR protocol.** Real-time PCR amplification reactions were carried out in a final volume
156 of 20 µl of reaction mixture containing 10 µl of Takyon NoRox Probe MasterMix dTTP (Eurogentec),
157 0.45 µM (each) primers, 0.45 µM labeled probe and 5 µl of purified DNA. Amplification was
158 performed using a Bio-Rad CFX96 platform and the following cycling parameters: heating at 50°C for
159 two minutes and 95°C for three minutes, followed by 45 cycles of a two-stage temperature profile of
160 95°C for three seconds and 60°C for 30 seconds.

161 **Evaluation of the sensitivity and specificity of the *Kkimdh* RT-PCR assay.** Twenty *K. kingae* strains
162 belonging to 20 distinct sequence types (STs) (Table S2) which had previously tested positive for
163 *KkigroEL*, *rtxA*, and *rtxB* [15], and 96 specimens which had previously tested positive for *KkigroEL*
164 were tested using the *Kkimdh*-RT-PCR assay. In addition, 105 various *KkigroEL*-negative clinical
165 specimens derived from children with suspected osteoarticular infections were added to the analysis.
166 Furthermore, 87 other bacterial strains, including strains from *K. negevensis*, *K. oralis*, *K. denitrificans*
167 and *K. potus*, as well as members of the *Neisseria*, *Haemophilus*, *Staphylococcus*, *Streptococcus* and
168 *Mycobacterium* genera were tested to assess the specificity of the assay (Table S2). To determine the
169 detection limit of the method, 12-fold serial dilutions of a bacterial suspension of *K. kingae* strain
170 ATCC 23330^T at an initial concentration of 10⁸ bacteria ml⁻¹ in phosphate-buffered saline were
171 evaluated and further quantified by culture on 5% sheep blood-enriched Columbia agar (bioMérieux)
172 and colony counting.

173 **Ethics statement.** This study was approved by the Ethics Committee of the IHU Méditerranée-
174 Infection under reference number 2017-006. Epidemiological studies performed in the 2000s were
175 approved by the Ethics Committee of the Soroka University Medical Center, as well as by the Israel
176 Ministry of Health.

177 **Accession number(s).** The GenBank accession numbers for the *mdh* genes from the 45 studied *K.*
178 *kingae* strains analyzed in this study are LT985480 to LT985524 (Table S1).

179

180

181 **RESULTS**

182 **Genomic analysis of the *mdh* gene of *K. kingae* and its environment.** A 978-bp *Kkimdh* gene was
183 identified in all 45 *K. kingae* genomes. The chromosomal region carrying the *Kkimdh* gene is
184 surrounded by the ribosomal small subunit-dependent GTPase gene located 218 bp upstream, and
185 downstream by a locus containing genes coding for the GTP cyclohydrolase FOLE2 and sensor
186 histidine kinase (Fig. 1). The synteny of this genomic architecture was conserved in all 45 *K. kingae*
187 strains. The distance matrix calculated from the 45 *Kkimdh* DNA sequences displayed 18 distinct
188 variants (Fig. 2), with a maximum distance of 98.4% between *K. kingae* strains ATCC 23330^T and
189 D2363 (Table S4).

190 ***In silico* analysis of the *Kkimdh* gene and design of the *Kkimdh*-specific RT-PCR assay.** The
191 Megablastn search indicated the presence of a *mdh* gene within the genomes of *Acinetobacter*
192 *woffii* ZS207 (CP019143), *Acidovorax* sp. RAC01 (CP016447), *Neisseria* sp. KEM232 (CP022527.1),
193 *Neisseria elongata* subsp. *glycolytica* ATCC 29315 (CP007726.1), *Neisseria weaveri* NCTC13585
194 (LT90643.1), *Neisseria zoodegmatis* NCTC12230 (LN869922.1), and *Polaromonas naphthalenivorans*
195 CJ2 (CP000529). The MAFFT alignment of the nucleotide sequences of these *mdh* orthologous genes
196 showed that the *Kkimdh*-F and *Kkimdh*-R primers, and the *Kkimdh*-P probe displayed a total of 13 to
197 15 mismatches between the *mdh* genes from *K. kingae* ATCC 23330^T and those from the *Neisseria*
198 species, which are the closest orthologous genes related to *Kkimdh* by showing nucleotide sequences
199 identities ranging from 77.1 to 79.1% (Fig. S1, Table S5). These data thereby demonstrate a high
200 index of *in silico* specificity of *Kkimdh*-RT-PCR assay.

201 **Validation of the *Kkimdh*-specific RT-PCR assay.** The detection threshold of the *Kkimdh* RT-PCR assay
202 was determined to be 10 CFU/ml. The assay was positive for all 20 *K. kingae* strains belonging to 20
203 distinct STs, whereas no amplification was obtained for *K. negevensis*, *K. denitrificans*, *K. oralis* and *K.*
204 *potus* strains (Table 1). Similarly, no amplification was obtained from any of the other 82 tested
205 bacterial species. As expected, *Kkimdh*-specific RT-PCR testing was positive in the 96 *KkigroEL*-
206 positive specimens. Unexpectedly, eight joint fluid samples initially tested *KkigroEL*-negative were

207 detected *Kkimdh*-positive, whereas the remaining 97 *KkigroEL*-negative pediatric specimens were
208 both *Kkimdh*-and *KkigroEL*-negative. Triplicate assays were carried out on the eight discrepant
209 samples. All eight were repeatedly *Kkimdh*-positive, with cycle threshold values ranging from 30 to
210 34. Of these eight *Kkimdh*-positive clinical specimens, six were derived from children with septic
211 arthritis aged between seven and 29 months, one was sampled from the oropharynx of a 13-month-
212 old boy, and one was identified in the joint fluid of a seven-year-old boy (Table S3).

213

214

215 **DISCUSSION**

216 This study reports a novel *K. kingae*-specific RT-PCR assay targeting the *Kkimdh* gene, a housekeeping
217 gene coding the malate dehydrogenase that was identified in 45 distinct *K. kingae* genomes, and
218 firmly detected in 20 various clinical isolates and 104 clinical specimens from infants and young
219 children originally from Europe, South America, Africa and the South Pacific. The high specificity of
220 this PCR system was demonstrated by the absence of any *mdh* gene in the genomes of all other
221 *Kingella* species. In addition, orthologous *mdh* genes were found in only a few bacterial species,
222 which exhibited low levels of nucleotide identity with *Kkimdh*, as demonstrated by the presence of
223 13 to 15 mismatches between the nucleotide sequences of primers and probe Fwd-Kkimdh, Rev-
224 Kkimdh, P-Kkimdh, and orthologous *mdh* genes from *Neisseria* species.

225 In contrast to the *Kingella* sp. RTX locus, *Kkimdh* is only present in *K. kingae*, is located in a genomic
226 region that presents a conserved synteny and a GC content of only 2 to 3% greater than that the
227 whole genome of *K. kingae*, and is not surrounded by transposable elements. For all these reasons, it
228 appeared particularly pertinent to target *Kkimdh* for the development of a new *K. kingae*-specific
229 molecular tool in clinical microbiology.

230 To the best of our knowledge, this new *K. kingae*-specific RT-PCR assay is currently the only
231 molecular tool showing optimal sensitivity and specificity for the diagnosis of *K. kingae* infection and
232 carriage when compared to all those previously reported. Although *K. kingae*-specific RT-PCR assays

233 targeting the *groEL* gene may be considered as the gold standard for the detection of *K. kingae*
234 [15,22], primers and probes reported by Ilharreborde *et al.* and Levy *et al.* may present between one
235 and three mismatches with *KkingroEL* nucleotide sequences from *K. kingae* isolates belonging to STc-6
236 and -35 (data not shown), which are two STcs previously shown to be responsible for invasive
237 infections in pediatrics [35], and which may impact the degree of sensitivity of these RT-PCR tests
238 [15,23]. Although mismatches in primer regions may have a limited effect on the quality of the
239 amplification curves, they may result in a significant increase in cycle threshold values [36,37]. Two
240 mismatches can delay amplification by three to five cycles, while three mismatches can delay
241 amplification by seven to 13 cycles [37]. In addition, single mismatches in the minor groove binding-
242 modified probes may result in no or weak amplification curves leading to the risk of being
243 interpreted as negative [38]. Because *K. kingae*-positive clinical specimens commonly contain a low
244 bacterial load, a highly sensitive molecular tool is, therefore, of significant importance to maximize
245 the detection yield of the organism from paucibacillary specimens.

246 Regarding the RT-PCR assays targeting the RTX locus, it was recently demonstrated that such
247 molecular tools are not valid to formally confirm the diagnosis of *K. kingae* infection because of the
248 cross-detection with *K. negevensis* [15]. In addition, given the numerous uncharacterized microbes
249 colonizing humans [39], and the multiple genomic factors indicating that the *Kingella* sp. RTX locus
250 was horizontally acquired, such as *ISKne1*, a *Kingella* sp. RTX locus-related transposable element
251 found in multiple copies in both *K. negevensis* and *K. kingae* genomes [15], it cannot be entirely ruled
252 out that a similar *Kingella* sp. RTX locus may have been transferred to other as yet uncharacterized
253 *Kingella* species. Consequently, this implies that the numerous studies conducted over the past
254 decade to calculate the prevalence rate of *K. kingae* infection and carriage using *Kingella* sp. RTX-
255 related molecular methods are likely to have, unintentionally, overestimated the results.

256 To overcome the lack of specificity of RT-PCRs assays targeting the *Kingella* sp. RTX locus and to
257 distinguish *K. kingae* from *K. negevensis* in clinical samples, Opota *et al.* recently proposed a strategy
258 which consists in targeting both *KkingroEL* and *Kingella* sp. *rtxA* by using a duplex RT-PCR assay for

259 diagnosing *K. kingae* infection [25]. Such a diagnostic strategy is strongly debatable and comprises
260 serious limitations for its use in the clinical diagnostic setting. Indeed, the genomic nature of the RTX
261 locus from *Kingella* sp. makes its lateral transfer in uncharacterized *Kingella* species possible. More
262 importantly, while *K. kingae* and *K. negevensis* share the same oropharyngeal niche and may
263 potentially be involved in pediatric osteoarticular infections, this duplex RT-PCR assay does not make
264 it possible to diagnose potential dual infections, or carriage caused by both *K. kingae* and *K.*
265 *negevensis* [Pablo Yagupsky, unpublished data].

266 Recently, de Knecht *et al.* developed a similar approach to diagnose osteoarticular infections caused
267 by *K. kingae* in a Danish pediatric population, after designing new primers and probes against the
268 *rtxA* gene to maximize sensitivity and optimizing the *KkigroEL*-specific RT-PCR assay reported by
269 Ilharreborde *et al.* [23]. Interestingly, 12 specimens were *Kingella* sp. *rtxA*-positive, and only 10 were
270 positive for both *rtxA* and *groEL*. The authors suggested that the two *rtxA*-positive and *KkigroEL*-
271 negative specimens may be explained by a positivity near the limit of detection of their two RT-PCR
272 tests, a sampling error, or decreased sensitivity due to mismatches of either primers or probes in the
273 *KkigroEL* gene. Nevertheless, because it was previously demonstrated that *K. negevensis*, which is
274 *rtxA*- and *rtxB*-positive and *KkigroEL*-negative, may occasionally induce joint infections in infancy,
275 such findings in Denmark may be consistent with infections caused by *K. negevensis*, as previously
276 observed in France [15].

277 Therefore, as there is currently a lack of clinical data regarding *K. negevensis*, being able to formally
278 discriminate *K. kingae* from *K. negevensis* is important. As a consequence, the development of highly
279 species-specific and sensitive RT-PCR assays emerges as the most effective and reliable diagnostic
280 strategy in clinical microbiology. Recently, the development of a *K. negevensis*-specific RT-PCR testing
281 targeting the *K. negevensis groEL* gene enabled identification of the first arthritis caused by *K.*
282 *negevensis* in an eight-month boy [15]. To diagnose infections and carriage caused by *K. kingae*, the
283 new *Kkimdh*-specific RT-PCR assay that we describe herein thereby appears as an optimal molecular
284 tool that could be used either alone, or in combination with *K. negevensis*-specific RT-PCR assays.

285 However, it should be emphasized that such RT-PCR assays remain costly, and that dual target PCR is
286 particularly advantageous to compensate for the potentially decreased sensitivity of assays applying
287 minor groove-binding probes [38]. Given that no target variation in the *Kkimdh* gene was detected in
288 a large and diverse collection of *K. kingae* strains, the *Kkimdh*-related primers and probe designed in
289 the present study appear to be robust enough to be applied alone in the clinical diagnostic setting.

290

291 **ACKNOWLEDGEMENTS**

292 The study was funded by the Foundation Méditerranée Infection and the French National Research
293 Agency under the program “Investissements d’avenir”, reference ANR-10-IAHU-03. The authors
294 would like to gratefully acknowledge Prof. Pablo Yagupsky, microbiologist at the Clinical Microbiology
295 Laboratory, Soroka Medical Center, Beer-Sheva, Israel, for providing numerous *K. kingae* isolates,
296 and for having critically reviewed this manuscript.

297

298

299

300 **REFERENCES**

- 301 1. Yagupsky P. 2015. *Kingella kingae*: carriage, transmission, and disease. Clin Microbiol Rev
302 28:54–79.
- 303 2. Yagupsky P, El Houmami N, Fournier PE. 2017. Outbreaks of Invasive *Kingella kingae* Infections in
304 Daycare Facilities: Approach to Investigation and Management. J Pediatr 182:14–20.
- 305 3. Fournier PE, Drancourt M, Colson P, Rolain JM, La Scola B, Raoult D. 2013. Modern clinical
306 microbiology: new challenges and solutions. Nat Rev Microbiol 11:574–585.
- 307 4. Ilharberorde B, Bidet P, Lorrot M, Even J, Mariani-Kurkdjian P, Liguori S, Vitoux C, Lefevre Y, Doit C,
308 Fitoussi F, Penneçot G, Bingen E, Mazda K, Bonacorsi S. 2009. New real-time PCR-based method
309 for *Kingella kingae* DNA detection: application to samples collected from 89 children with acute
310 arthritis. J Clin Microbiol 47:1837–1841. Erratum in: 2009. J Clin Microbiol 47:3071.
- 311 5. Levy PY, Fournier PE, Fenollar F, Raoult D. 2013. Systematic PCR detection in culture-negative
312 osteoarticular infections. Am J Med 126:1143.e25–33.
- 313 6. Chometon S, Benito Y, Chaker M, Boisset S, Ploton C, Bérard J, Vandenesch F, Freydiere AM. 2007.
314 Specific real-time polymerase chain reaction places *Kingella kingae* as the most common cause of
315 osteoarticular infections in young children. Pediatr Infect Dis J 26:377–381.
- 316 7. El Houmami N, Yagupsky P, Ceroni D. 2018. *Kingella kingae* hand and wrist tenosynovitis in young
317 children. J Hand Surg Eur Vol. Jan 1:1753193418764818.
- 318 8. Juchler C, Spyropoulou V, Wagner N, Merlini L, Dhoub A, Manzano S, Tabard-Fougère A, Samara E,
319 Ceroni D. 2018. The Contemporary Bacteriologic Epidemiology of Osteoarticular Infections in
320 Children in Switzerland. J Pediatr 194:190-196.e1.
- 321 9. Ceroni D, Belaieff W, Cherkaoui A, Lascombes P, Schrenzel J, de Coulon G, Dubois-Ferrière V, Dayer
322 R. 2014. Primary epiphyseal or apophyseal subacute osteomyelitis in the pediatric population: a
323 report of fourteen cases and a systematic review of the literature. J Bone Joint Surg Am
324 96:1570–1575.

- 325 10. Ceroni D, Dubois-Ferrière V, Anderson R, Combescure C, Lamah L, Cherkaoui A, Schrenzel J. 2012.
326 Small risk of osteoarticular infections in children with asymptomatic oropharyngeal carriage of
327 *Kingella kingae*. *Pediatr Infect Dis J* 31:983–985.
- 328 11. Ceroni D, Dubois-Ferriere V, Cherkaoui A, Gesuele R, Combescure C, Lamah L, Manzano S, Hibbs J,
329 Schrenzel J. 2013. Detection of *Kingella kingae* osteoarticular infections in children by oropharyngeal
330 swab PCR. *Pediatrics* 131:e230–235.
- 331 12. Ceroni D, Llana RA, Kherad O, Dubois-Ferriere V, Lascombes P, Renzi G, Lamah L, Manzano S,
332 Cherkaoui A, Schrenzel J. 2013. Comparing the oropharyngeal colonization density of *Kingella kingae*
333 between asymptomatic carriers and children with invasive osteoarticular infections. *Pediatr Infect*
334 *Dis J* 32:412–414.
- 335 13. Verdier I, Gayet-Ageron A, Ploton C, Taylor P, Benito Y, Freydiere AM, Chotel F, Bérard
336 J, Vanhems P, Vandenesch F. 2005. Contribution of a broad range polymerase chain reaction to the
337 diagnosis of osteoarticular infections caused by *Kingella kingae*: description of twenty-four recent
338 pediatric diagnoses. *Pediatr Infect Dis J* 24:692–696.
- 339 14. Morel AS, Dubourg G, Prudent E, Edouard S, Gouriet F, Casalta JP, Fenollar F, Fournier PE,
340 Drancourt M, Raoult D. 2015. Complementarity between targeted real-time specific PCR and
341 conventional broad-range 16S rDNA PCR in the syndrome-driven diagnosis of infectious diseases. *Eur*
342 *J Clin Microbiol Infect Dis* 34:561–570.
- 343 15. El Houmami N, Bzdrenga J, Durand GA, Minodier P, Seligmann H, Prudent E, Bakour S, Bonacorsi
344 S, Raoult D, Yagupsky P, Fournier PE. 2017. Molecular Tests That Target the RTX Locus Do Not
345 Distinguish between *Kingella kingae* and the Recently Described *Kingella negevensis* Species. *J Clin*
346 *Microbiol* 55:3113–3122.
- 347 16. Cherkaoui A, Ceroni D, Emonet S, Lefevre Y, Schrenzel J. 2009. Molecular diagnosis
348 of *Kingella kingae* osteoarticular infections by specific real-time PCR assay. *J Med Microbiol*
349 58:65–68.

- 350 17. Lehours P, Freydière AM, Richer O, Burucoa C, Boisset S, Lanotte P, Prère MF, Ferroni A, Lafuente
351 C, Vandenesch F, Mégraud F, Ménard A. 2011. The *rtxA* toxin gene of *Kingella kingae*: a pertinent
352 target for molecular diagnosis of osteoarticular infections. *J Clin Microbiol* 49:1245–1250.
- 353 18. Links MG, Dumonceaux TJ, Hemmingsen SM, Hill JE. 2012. The chaperonin-60 universal target is a
354 barcode for bacteria that enables de novo assembly of metagenomics data. *Plos One* 7:e49755.
- 355 19. Chaban B, Hill JE. 2012. A 'universal' type II chaperonin PCR detection system for the investigation
356 of Archae in complex microbial communities. *ISME J* 6:430–439.
- 357 20. Olson AB, Sibley CD, Schmidt L, Wilcox MA, Surette MG, Corbett CR. 2010. Development of real-
358 time PCR assays for detection of the *Streptococcus milleri* group from cystic fibrosis clinical
359 specimens by targeting the *cpn60* and 16S rRNA genes. *J Clin Microbiol* 48:1150–1160.
- 360 21. Chaban B, Musil KM, Himsworth CG, Hill JE. 2009. Development of *cpn60*-based real-time
361 quantitative PCR assays for the detection of 14 *Campylobacter* species and application to screening
362 of canine fecal samples. *Appl Environ Microbiol* 75:3055–3061.
- 363 22. El Houmami N, Fournier PE, Ceroni D. 2017. Targeting the *Kingella Kingae* groEL gene is a reliable
364 method for the molecular diagnosis of *K. Kingae* infection and carriage. *J Paediatr Child Health*
365 53:1030–1031.
- 366 23. de Knecht VE, Kristiansen GQ, Schønning K. 2017. Evaluation of dual target-specific real-time PCR
367 for the detection of *Kingella kingae* in a Danish paediatric population. *Infect Dis (Lond)* 15:1–7.
- 368 24. Kehl-Fie TE, St Geme JW 3rd. 2007. Identification and characterization of an RTX toxin in the
369 emerging pathogen *Kingella kingae*. *J Bacteriol* 189:430–436.
- 370 25. Opota O, Laurent S, Pillonel T, Léger M, Trachsel S, Prod'hom G, Jaton K, Greub G. 2017.
371 Genomics of the new species *Kingella negevensis*: diagnostic issues and identification of a locus
372 encoding a RTX toxin. *Microbes Infect* 19:546–552.
- 373 26. El Houmami N, Bakour S, Bzdrenga J, Rathored J, Seligmann H, Robert C, Armstrong N, Schrenzel
374 J, Raoult D, Yagupsky P, Fournier PE. 2017. Isolation and characterization of *Kingella negevensis* sp.

375 nov., a novel *Kingella* species detected in a healthy paediatric population. Int J Syst Evol Microbiol
376 67:2370–2376.

377 27. El Houmami N, Schrenzel J, Yagupsky P, Robert C, Ceroni D, Raoult D, Fournier PE. 2017. Draft
378 Genome Sequence of *Kingella negevensis* SW7208426, the First European Strain of *K.*
379 *negevensis* Isolated from a Healthy Child in Switzerland. Genome Announc 5(26).

380 28. Yagupsky P, Merires M, Bahar J, Dagan R. 1995. Evaluation of novel vancomycin-containing
381 medium for primary isolation of *Kingella kingae* from upper respiratory tract specimens. J Clin
382 Microbiol 33:1426–1427.

383 29. Bidet P, Basmaci R, Guglielmini J, Doit C, Jost C, Birgy A, Bonacorsi S. 2015. Genome Analysis
384 of *Kingella kingae* Strain KWG1 Reveals How a β -Lactamase Gene Inserted in the Chromosome of
385 This Species. Antimicrob Agents Chemother 60:703–708.

386 30. Fournier PE, Rouli L, El Karkouri K, Nguyen TT, Yagupsky P, Raoult D. 2012. Genomic comparison
387 of *Kingella kingae* strains. J Bacteriol 194:5972.

388 31. Rouli L, Robert C, Raoult D, Yagupsky P. 2014. *Kingella kingae* KK247, an Atypical Pulsed-Field Gel
389 Electrophoresis Clone A Strain. Genome Announc 2(6).

390 32. Kearse M, Moir R, Wilson A, Stones-Havas S, Cheung M, Sturrock S, Buxton S, Cooper A,
391 Markowitz S, Duran C, Thierer T, Ashton B, Mentjies P, Drummond A. 2012. Geneious Basic: an
392 integrated and extendable desktop software platform for the organization and analysis of sequence
393 data. Bioinformatics 28:1647–1649.

394 33. Katoh K, Misawa K, Kuma K, Miyata T. 2002. MAFFT: a novel method for rapid multiple sequence
395 alignment based on fast Fourier transform. Nucleic Acids Res 30:3059–3066.

396 34. Kumar S, Stecher G, Tamura K. 2016. MEGA7: Molecular Evolutionary Genetics Analysis version
397 7.0 for bigger datasets. Mol Biol Evol 33:1870–1874.

398 35. Amit U, Porat N, Basmaci R, Bidet P, Bonacorsi S, Dagan R, Yagupsky P. 2012. Genotyping of
399 invasive *Kingella kingae* isolates reveals predominant clones and association with specific clinical
400 syndromes. Clin Infect Dis 55:1074–1079.

- 401 36. Bourhy P, Bremont S, Zinini F, Giry C, Picardeau M. 2011. Comparison of real-time PCR assays for
402 detection of pathogenic *Leptospira* spp. in blood and identification of variations in target sequences.
403 *J Clin Microbiol* 49:2154–2160.
- 404 37. Whiley DM, Sloots TP. 2005. Sequence variation in primer targets affects the accuracy of viral
405 quantitative PCR. *J Clin Virol* 34:104–107.
- 406 38. Kamau E, Agoti CN, Lewa CS, Oketch J, Owor BE, Otieno GP, Bett A, Cane PA, Nokes DJ. 2017.
407 Recent sequence variation in probe binding site affected detection of respiratory syncytial
408 virus group B by real-time RT-PCR. *J Clin Virol* 88:21–25.
- 409 39. Kowarsky M, Camunas-Soler J, Kertesz M, De Vlaminc I, Koh W, Pan W, Martin L, Neff
410 NF, Okamoto J, Wong RJ, Kharbanda S, El-Sayed Y, Blumenfeld Y, Stevenson DK, Shaw GM, Wolfe
411 ND, Quake SR. 2017. Numerous uncharacterized and highly divergent microbes which colonize
412 humans are revealed by circulating cell-free DNA. *Proc Natl Acad Sci USA* 114:9623–9628.
- 413 40. Saitou N, Nei M. 1987. The neighbor-joining method: A new method for reconstructing
414 phylogenetic trees. *Mol Biol and Evol* 4:406-425.
- 415 41. Tamura K, Nei M, and Kumar S. 2004. Prospects for inferring very large phylogenies by using the
416 neighbor-joining method. *Proc Natl Acad Sci USA* 101:11030–11035.

417

418 **FIGURE LEGENDS**

419 **Figure 1.** Genomic architecture of the region carrying the *mdh* gene of *Kingella kingae* (*Kkimdh*). The
420 genomic elements are not drawn to scale. The dashed lines indicate that the sensor histidine kinase
421 may be coded by either a single gene or two-component genes.

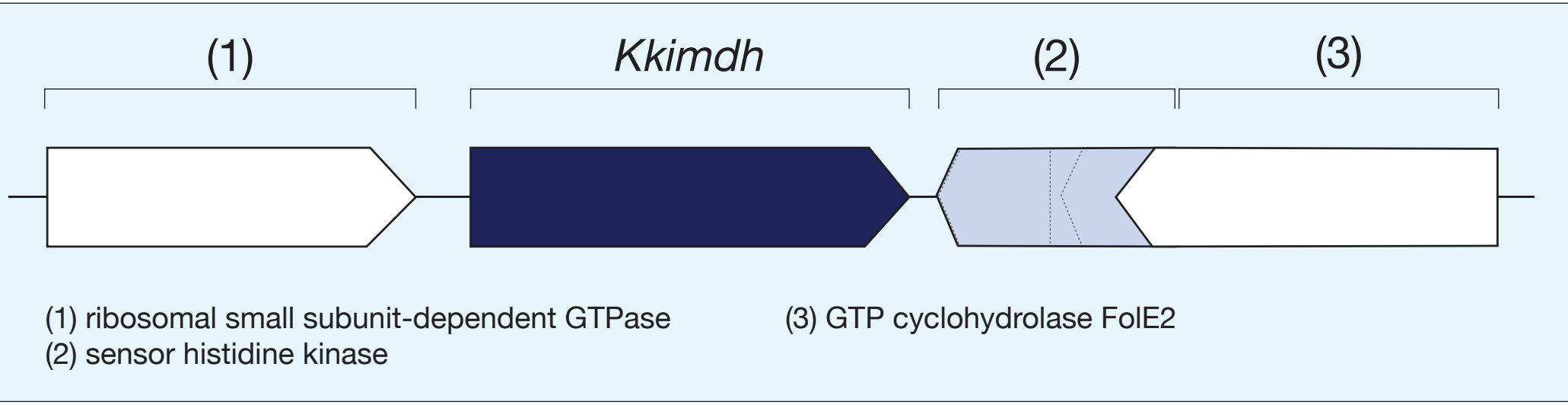
422 **Figure 2.** Neighbor-joining tree [40] based on the comparison of *mdh* nucleotide sequences from 18
423 genetic variants of *Kingella kingae* and its closest orthologs in *Acinetobacter*, *Acidovorax*,
424 *Polaromonas*, and *Neisseria* species. The tree is drawn to scale, with branch lengths in the same units
425 as those of the evolutionary distances used to infer the phylogenetic tree. The evolutionary distances
426 were computed using the Maximum Composite Likelihood method [41] and are in the units of the

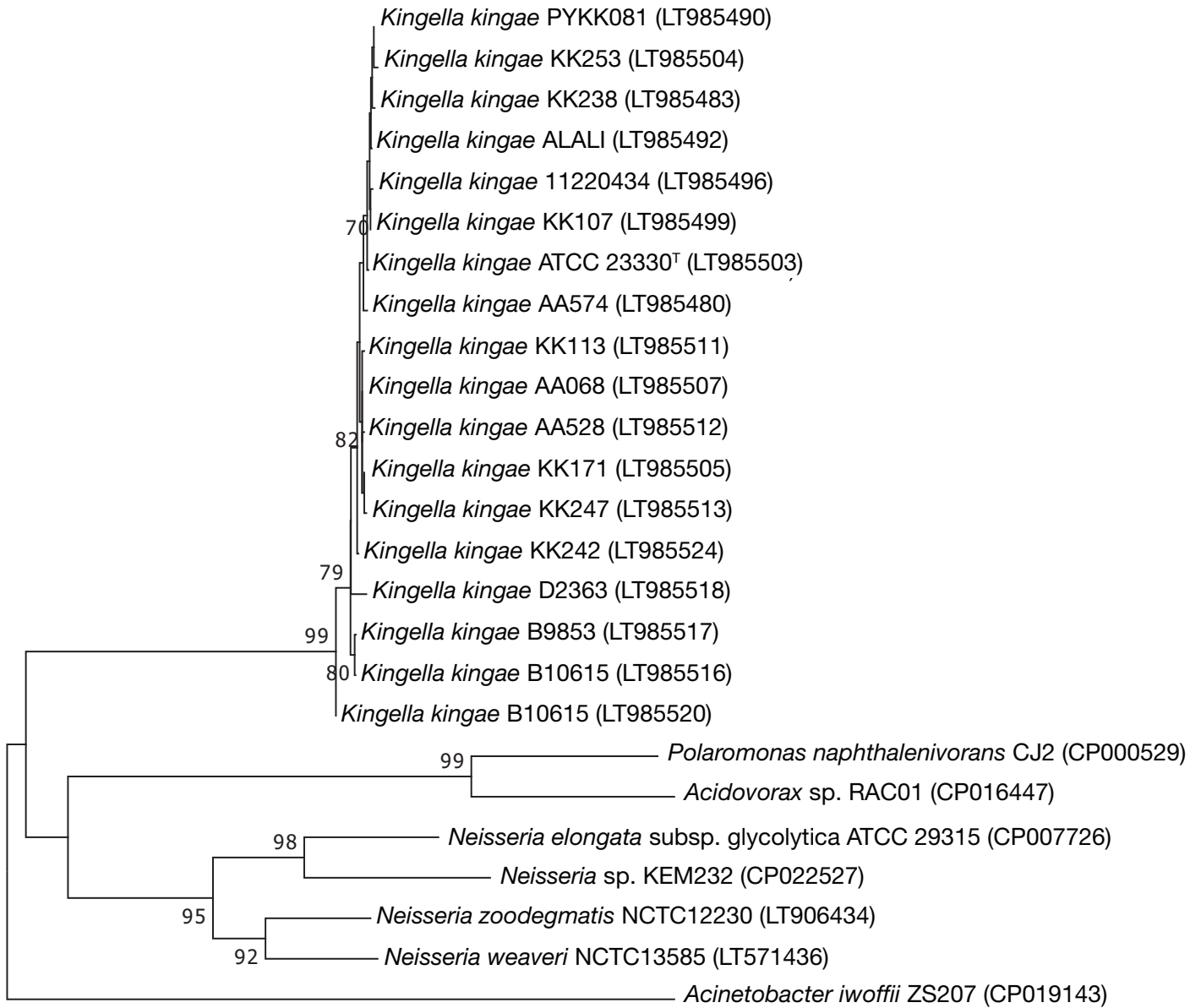
427 number of base substitutions per site. The scale bar indicates a 10% nucleotide sequence divergence.
428 Bootstrap values (expressed as percentages of 1,000 replications) are showed next to the branches.
429 Only bootstrap values greater than or equal to 70% were displayed. All positions containing gaps and
430 missing data were eliminated. There was a total of 978 positions in the final dataset.

431

432 **TABLE LEGENDS**

433 **Table 1.** Results of the real-time PCR assays targeting the *groEL* and *mdh* genes of *K. kingae* (*KkigroEL*
434 and *Kkimdh*) that were tested on 20 genotypically distinct *K. kingae* isolates, and 201 paediatric
435 specimens.





0.1

Table 1. Results of the real-time PCR assays targeting the *groEL* and *mdh* genes of *K. kingae* (*KkigroEL* and *Kkimdh*) that were tested on 20 genotypically distinct *K. kingae* isolates, and 201 paediatric specimens.

	<i>Kkimdh</i> -positive	<i>KkigroEL</i> -positive
<i>K. kingae</i> isolates (n=20)	20	20
Other bacterial species (n=86)	0	0
Clinical specimens (n=201)*		
Initially <i>KkigroEL</i> -positive (n=96)	96	96
Initially <i>KkigroEL</i> -negative (n=105)	8	0

* Patients were tested for a suspected *K. kingae* invasive infection.